Chemical Science

ROYAL SOCIETY OF CHEMISTRY

EDGE ARTICLE

View Article Online
View Journal | View Issue

Cite this: *Chem. Sci.*, 2022, **13**, 12469

All publication charges for this article have been paid for by the Royal Society of Chemistry

Received 21st July 2022
Accepted 12th October 2022

DOI: 10.1039/d2sc04078f

rsc.li/chemical-science

Chain transfer agents for the catalytic ring opening metathesis polymerization of norbornenes†‡

Indradip Mandal, Ankita Mandal, Md Atiur Rahman and Andreas F. M. Kilbinger *

Here, we present a detailed study of the metathesis activity of conjugated 1,3 diene derivatives in ring opening metathesis polymerization (ROMP) using Grubbs' 3rd generation catalyst (**G3**). A comprehensive screening of those derivatives revealed that monosubstituted 1,3 dienes show similar reactivities towards G3-alkylidenes as norbornene derivatives. Therefore, they represent perfect candidates for chain transfer agents in a kinetically controlled catalytic ROMP. This unprecedented reactivity allowed us to catalytically synthesize mono-end-functional poly(norborneneimide)s on the gram scale. Much more complex architectures such as star-shaped polymers could also be synthesized catalytically for the very first time *via* ROMP. This inexpensive and greener route to produce telechelic ROMP polymers was further utilized to synthesize ROMP block copolymers using bifunctional ROMP and ATRP/NCL initiators. Finally, the regioselective reaction of **G3** with 1,3 diene derivatives was also exploited in the synthesis of a ROMP-PEG diblock copolymer initiated from a PEG macroinitiator.

Introduction

Over the last few decades, ring opening metathesis polymerization (ROMP) has emerged as a powerful polymerization technique to produce highly functional and diverse materials.[1] Typical metathesis initiators for ROMP are based on ruthenium[2] and molybdenum[3] complexes. Among these, commercially available ruthenium-based complexes discovered by Grubbs' and coworkers are often preferred due to their robustness and excellent tolerance toward many functional groups.[4] Grubbs' 2nd generation catalyst (**G2**) and Grubbs' 3rd generation catalyst (**G3**) are frequently used for polymerizations.[5–7] The mechanism of ROMP involves a chain-growth polymerization where a strained cyclic olefin (monomer) is converted to a polymeric species.[8] The high functional group tolerance of Grubbs' catalysts allowed the synthesis of telechelic ROMP polymers[9–15] that has great importance in many disciplines of chemistry.

Based on the choice of monomers, ROMP, in general, can either be catalytic or stoichiometric in the ruthenium complex (Scheme 1). For example, polymerization of cyclooctene and its derivatives or unsubstituted norbornene can be carried out with catalytic amounts of ruthenium carbene complexes using irreversible symmetrical chain transfer agents (CTAs) under thermodynamically controlled conditions.[16–19] This method heavily relies on "backbiting" to produce homotelechelic polymers. Even though it reduces the loading of costly ruthenium catalysts, this method is restricted to very few monomers.

On the other hand, in a typical living ROMP where norbornene imide-based monomers are often used, equimolar amounts of metathesis catalyst are required with respect to the number of polymer chains formed, making the whole process non-catalytic. Our group recently addressed this issue utilizing a degenerative chain-transfer mechanism that used only catalytic amounts of ruthenium complex.[20,21] Although this new method is mechanistically unique; it is limited in terms of functional and readily available chain transfer agents. Pulsed monomer addition is another technique in ROMP to obtain telechelic polymers using a sub-stoichiometric amount of metal complex.[22–25] Lastly, a theoretically straightforward approach to synthesizing ROMP polymers is based on a kinetically controlled chain transfer mechanism. Katayama *et al.* reported true heterotelechelic ROMP polymers using functional vinyl ethers, vinyl thioethers, and vinyl acetates that undergo regioselective chain transfer.[26–28] Only norbornene was used as a monomer to give heterotelechelic poly(norbornene) in a kinetically controlled catalytic process. Therefore, this method is limited in terms of monomer scope.

Here, we report a new kinetically controlled chain transfer ROMP mechanism. We developed a new class of chain transfer agents containing monosubstituted 1,3 dienes to catalytically produce mono-end-functional poly(norborneneimide)s, bi, tri, and tetrafunctionally initiated linear and three and four-arm star polymers for the very first time in metathesis polymerization.

Department of Chemistry, University of Fribourg, Chemin du Musée 9, 1700 Fribourg, Switzerland. E-mail: andreas.kilbinger@unifr.ch

† This work is dedicated to the memory of Professor Robert H. Grubbs.

‡ Electronic supplementary information (ESI) available. See https://doi.org/10.1039/d2sc04078f

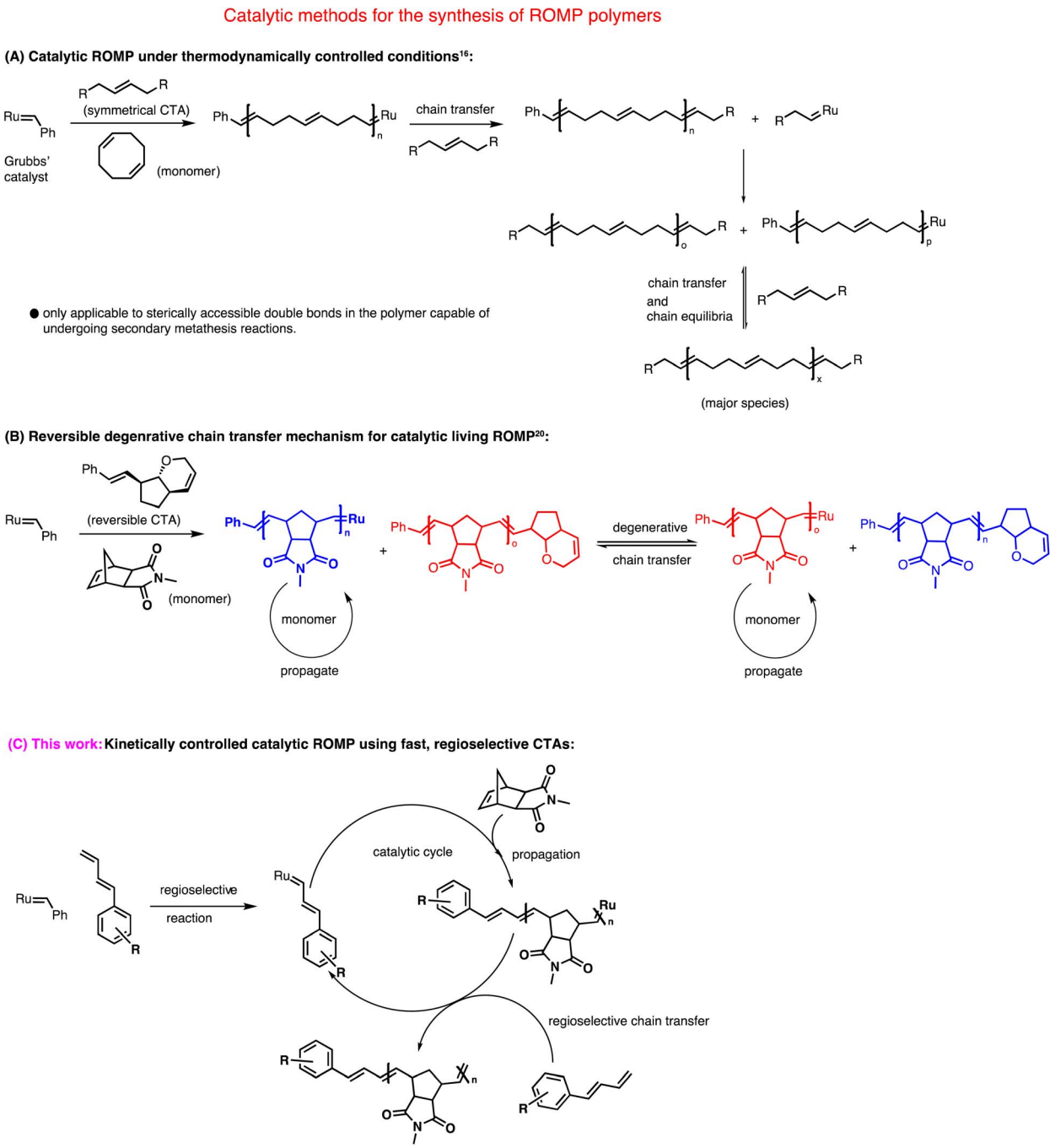

Scheme 1 Mechanistic illustration of three different approaches for the catalytic synthesis of ROMP polymers.

Results and discussion

Mono-end functional poly(norborneneimide)s *via* catalytic ROMP

Grubbs' Ru complexes react with electron-rich double bonds such as vinyl ethers in a regioselective manner.[29,30] We hypothesized that monosubstituted 1,3 diene compounds containing an electron-rich as well as the sterically accessible conjugated double bond (Scheme S1‡) would exhibit a similar fast, regioselective cross-metathesis reaction with **G3**. Therefore, a functional monosubstituted 1,3- diene (**CTA1**, Fig. 1) was synthesized in a few straightforward steps (see ESI‡).

To demonstrate our concept, **G3** (1 equiv.) and 1 equiv. of **CTA1** was dissolved in dichloromethane-d_2, added to an NMR tube and the reaction was followed by ^{1}H NMR spectroscopy (see Fig. S1‡). Within the first measurement (<10 min), the signals of the terminal double-bond (**CTA1**) (5.15 ppm and 5.32 ppm) disappeared along with the generation of new peaks at 5.25 ppm and 5.75 ppm, which corresponded to the formation of styrene.

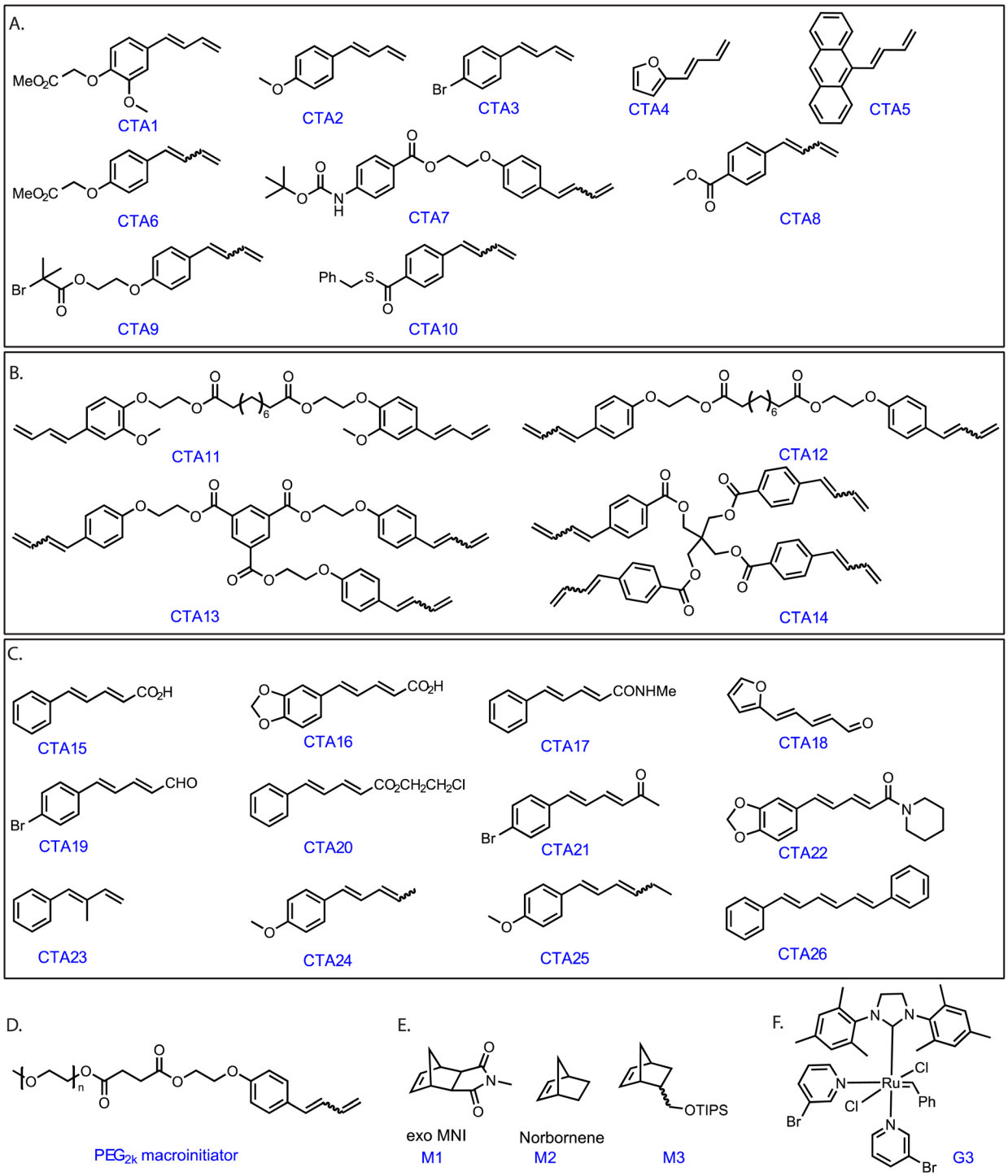

Fig. 1 Chemical structures of compounds investigated in this study: (A) monosubstituted, functional chain transfer agents (CTAs) (**CTA1–20**). (B) Bi, tri, and tetra functional CTAs (**CTA11–14**). (C) Disubstituted CTAs (**CTA15–26**). (D) poly(ethylene glycol) based macroinitiator (PEG_{2k} macroinitiator). (E) Structures of monomers. (F) Structure of Grubbs' 3rd generation catalyst (**G3**).

Moreover, looking at the ruthenium alkylidene region, we observed the formation of a new doublet at 18.56 ppm. As proposed, the ruthenium complex reacted regioselectively, forming an electronically stable conjugated carbene (thus, producing styrene) rather than the methylidene complex. The fact that only 1 equiv. **CTA1** could fully pre-functionalize commercial **G3** benzylidene indicated an unexpectedly high reactivity of the terminal conjugated double bond. Additionally, an end-capping experiment was performed where a **G3**-benzylidene initiated poly (exo-*N*-methyl norbornene imide, **M1**) (**M1 : G3** = 20) was end-capped with 1.2 equiv. of **CTA1** in an NMR tube. To our expectation, the complete disappearance of

the **G3**-alkylidene signal (at 18.45 ppm) and the formation of a doublet at 18.56 ppm and a doublet of doublet at 8.40 ppm were observed immediately, suggesting the formation of only one type of conjugated Ru complex (Fig. 2). This regioselective chain transfer was further confirmed by isotopically resolved MALDI-ToF MS analysis of the precipitated polymer (**P1**), showing a single set of mass distributions with expected polymer end groups: phenyl on one end (from **G3**) and methylene on the other (from **CTA1**, mono-isotopic mass: 4106.70 *vs.* observed mass: 4106.61, Fig. S3‡). Analysis of **P1** by size exclusion chromatography (SEC) showed a single, monomodal peak indicating absence of any chain end coupling products (Fig. S208‡). The exceptionally high metathesis reactivity of **CTA1** prompted us to investigate a catalytic ring opening metathesis polymerization that exploits a kinetically controlled chain transfer process. Next, we performed a one-pot polymerization using a ratio of **G3 : CTA1 : M1** = 1 : 40 : 400. SEC analysis of the resulting polymer revealed a monomodal distribution with the molecular weight very close to the **M1**/**CTA1** ratio (**P2**, $M_{n,\ M1/CTA1} = 2.0$ kDa *vs.* $M_{n,\ SEC\ (CHCl3)} = 2.6$ kDa) and dispersity of 1.77. This suggested a catalytic polymerization involving a very efficient chain transfer to **CTA1**. In this mechanism, a propagating polymer chain reacts regioselectively with a CTA to regenerate the initiating species while terminating the polymer chain irreversibly (Fig. 3A). For this mechanism to work optimally, the chain transfer and monomer propagation rate constants should be identical. Moreover, isotopically resolved MALDI-ToF MS analysis confirmed the polymer structure with both **CTA1** end groups: a functional aromatic ring and a methylene unit (Fig. 3B). The polymerization was repeated, varying the **M1** to **CTA1** ratio (**P3–5**) (Table S1‡). The resulting polymers showed a linear dependence between **M1**/**CTA1**, and the number average molecular weight (M_n) determined by SEC (Fig. 3C) indicating that excellent control over molecular weight could be obtained by this method. Next, a methoxy substituted **CTA2** was employed, and the **G3** to **CTA2** ratio was lowered to 1 : 300. A polymer with reasonable control over molecular weight (**P6**, $M_{n,\ M_1/CTA2} = 1.9$ kDa *vs.* $M_{n,\ SEC\ (CHCl_3)} = 2.5$ kDa) was obtained in high yield (91%). To the best of our knowledge, this is the lowest Ru-complex to CTA ratio ever employed to synthesize norbornene imide-based metathesis polymers. Then, **M1** was polymerized using **CTA3** (**P7**, **G3 : CTA3** = 1 : 100, $M_{n,\ SEC\ (CHCl3)} = 3.9$ kDa), **CTA3** (**P8**,**G3 : CTA3** = 1 : 50, $M_{n,\ SEC\ (CHCl_3)} = 44.0$ kDa), **CTA4** (**P9**, **G3 : CTA4** = 1 : 100, $M_{n,\ SEC\ (CHCl_3)} = 4.4$ kDa), and **CTA5** (**P10**, **G3 : CTA5** = 1 : 200, $M_{n,\ SEC\ (CHCl_3)} = 2.3$ kDa) (Table S1‡). The purified polymers were fully characterized using NMR spectroscopy and MALDI-ToF mass spectrometry. **P10** draws special attention here due to the ease at which our method introduced a fluorescent group (anthracene) to a polymer chain end. It is worth mentioning that there have been many attempts in ROMP to synthesize precisely labeled metathesis polymers, in particular, fluorescent labels, due to their applications in bioimaging, drug delivery, *etc.*[31,32]

To elucidate the proposed kinetically controlled mechanism in detail, a ^{1}H NMR kinetics experiment was performed taking **G3** (1 equiv.), **CTA3** (50 equiv.) and **M1** (1000 equiv.) in $CDCl_3$. 3-bromopyridine was added as an additive to slow down the polymerization, and thus, conversion of **M1** and **CTA3** were followed over time. A plot of conversion *vs.* time for **M1** and **CTA3** showed that both components of the polymerization mixture were consumed almost at the same rate during the polymerization (over 317 min) (Fig. 3D and S6‡). This strongly suggests a kinetically controlled mechanism for this type of CTA. To further elucidate the mechanism detailed kinetic study was performed and the rate of consumption of both monomer (**M1**) and CTA (**CTA3**) (see Fig. S263 and S264‡) were determined. Gratifyingly, rate constants obtained for both monomer consumption ($k_{M_1} = 0.01531\ min^{-1}$) and **CTA3** consumption ($k_{CTA3} = 0.01434\ min^{-1}$) are of a similar magnitude which was predicted for a kinetically controlled chain transfer mechanism.

Moreover, the effect of CTA concentration on the kinetics of polymerization was also exploited using ^{1}H NMR spectroscopy.

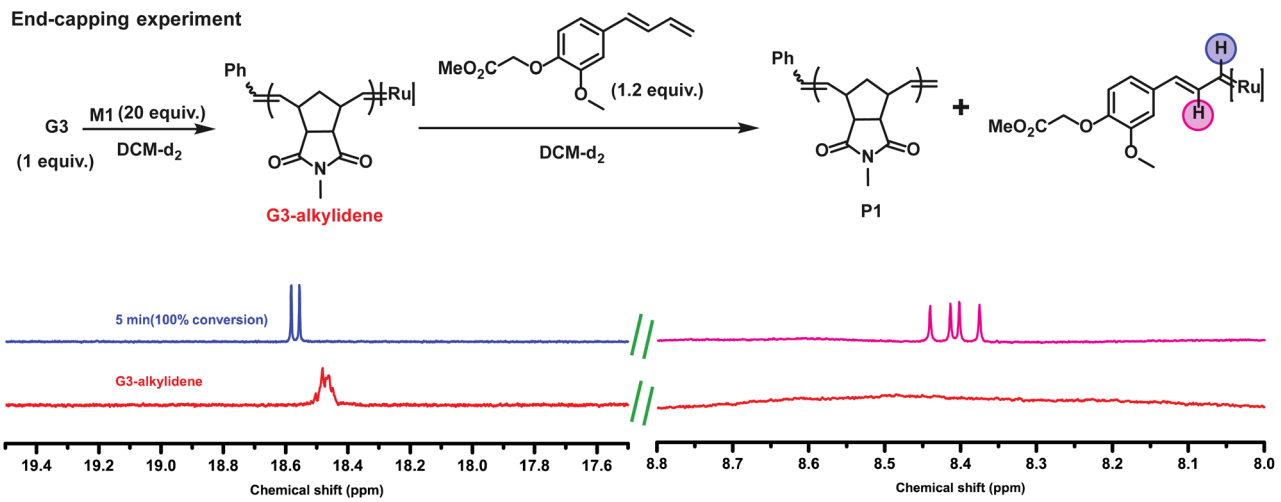

Fig. 2 ^{1}H NMR spectra (CD_2Cl_2, 400 MHz) showing the propagating **G3**-alkylidene complex (at 18.45 ppm, red line) and its reaction with only 1.2 equiv. of **CTA1** after 5 min (doublet at 18.56 ppm, in blue and doublet of doublet at 8.40 ppm, in magenta).

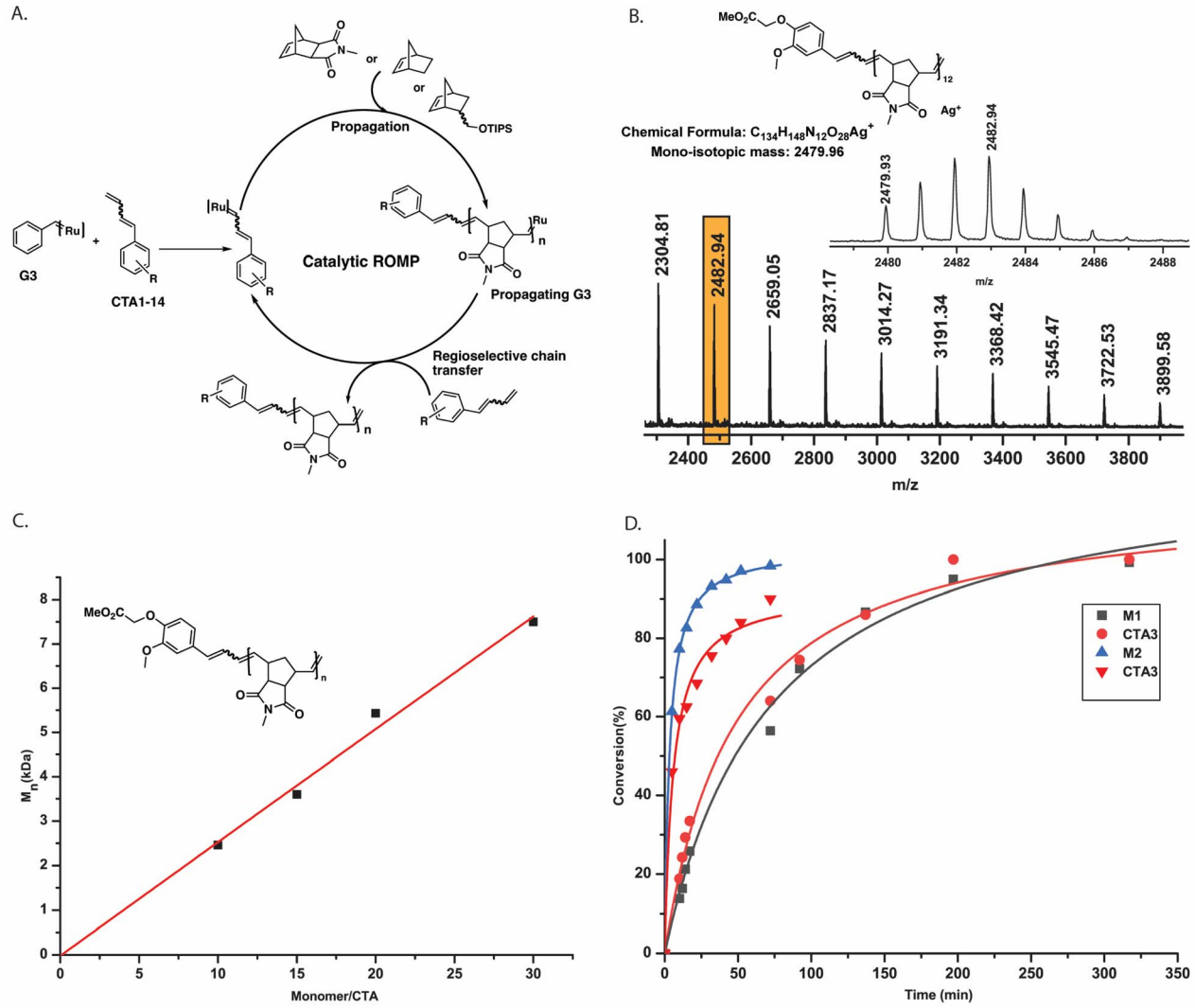

Fig. 3 Mechanistic details for the proposed kinetically controlled mechanism. (A) Mechanism of catalytic ROMP. **G3** catalyst reacts with CTA regioselectively to give a functional catalyst which, upon introduction of monomer (**M1** was used in the catalytic cycle as an example), produces a propagating **G3**. As the rate of chain transfer to the CTA is fast, the propagating **G3** reacts regioselectivity to give back the functional catalyst, which closes the catalytic cycle. (B) Isotopically resolved MALDI-ToF mass spectrum (DCTB, AgTFA) of the polymer **P2** matching the proposed end groups that resulted from **CTA1**. (C) A plot of the number average molecular weight (M_n) *versus* monomer to CTA ratio showing a linear correlation. Polymerizations were carried out with **M1**, **CTA1**, and **G3** under standard degassed conditions. M_n was measured using SEC in chloroform. (D) A plot of monomers (**M1** and **M2**, 1000 equiv.) and **CTA3** (50 equiv.) conversion *vs.* time determined by ^{1}H NMR spectroscopy ($CDCl_3$, 300 MHz) showing both monomer and CTA were consumed at a similar rate during the polymerization, thus, suggesting a kinetically controlled mechanism.

As expected for a chain transfer chain growth polymerization, rate of the reaction was inversely proportional to the concentration of the CTA (see Fig. S272 and Table S6‡).

In **CTA1–5**, the diene double bond was necessarily trans configured as their synthesis was based on *trans*-cinnamaldehyde derivatives. Only very few such derivatives are commercially available and thus limit the introduction of functionality in our CTAs. However, we envisioned that a CTA with a mixture of cis and trans double bonds could be synthesized easily from an aromatic aldehyde using allyl triphenylphosphonium bromide in a Wittig reaction. Thus, **CTA6–10** were prepared. A polymer end-capping experiment, as described above, was performed using **CTA6**, and the reaction was followed by ^{1}H NMR spectroscopy (Fig. S11‡). Although all the propagating poly(**M1**) alkylidene signals vanished immediately, several doublet peaks were observed in the ruthenium alkylidene region, presumably, due to the coordination of the cis double bond of **CTA6** to the ruthenium complex. Nonetheless, a clean MALDI-ToF mass spectrum (Fig. S12‡) with methylene terminated polymer chains confirmed the expected regioselectivity. Furthermore, **M1** was polymerized using **CTA6** (**P11**, **G3** : **CTA6** = 1 : 100, $M_{n,\,SEC\,(CHCl3)}$ = 6.5 kDa), **CTA8** (**P12**, **G3** : **CTA8** = 1 : 20, $M_{n,\,SEC\,(CHCl_3)}$ = 3.4 kDa), **CTA9** (**P13**, **G3** : **CTA9** = 1 : 100, $M_{n,\,SEC\,(CHCl3)}$ = 7.9 kDa), and **CTA10** (**P14**, **G3** : **CTA10** = 1 : 100, $M_{n,\,SEC\,(CHCl3)}$ = 5.0 kDa) (Table S1‡). All showed distinct end groups in the ^{1}H NMR

spectra and isotopically resolved MALDI ToF MS signals matching the two expected end groups (see ESI‡).

Norbornene (**M2**) is a highly strained monomer that has been studied immensely in ROMP. Norbornene propagates more rapidly than norborneneimide derivatives and is, therefore, more difficult to polymerize catalytically under kinetic control. Here, we have taken into account the very high reactivity of our CTAs and synthesized monotelechelic poly (norbornene) using a catalytic amount of Grubbs' initiator. For example, **CTA2** (**P15**, **G3 : CTA2** = 1 : 100, $M_{n,\ SEC\ (CHCl3)}$ = 7.2 kDa), **CTA5** (**P16**, **G3 : CTA5** = 1 : 100, $M_{n,\ SEC\ (CHCl3)}$ = 8.8 kDa), **CTA7** (**P17**, **G3 : CTA7** = 1 : 100, $M_{n,\ SEC\ (CHCl_3)}$ = 8.8 kDa), **CTA9** (**P18**, **G3 : CTA9** = 1 : 100, $M_{n,\ SEC\ (CHCl_3)}$ = 8.2 kDa), and **CTA10** (**P19**, **G3 : CTA10** = 1 : 170, $M_{n,\ SEC\ (CHCl3)}$ = 7.0 kDa) (Table S1‡) were employed to obtain poly(norbornene)s with excellent end group fidelity as observed by both ^{1}H NMR spectroscopy and MALDI-ToF mass spectrometry. The molecular weights of the poly(norbornene)s measured by SEC using $CHCl_3$ as eluent showed more than twice the theoretical value (see Table S2‡). However, monodisperse poly(styrene) samples were used as calibrants for SEC measurements, which have a different hydrodynamic radius compared to polydisperse poly(-norbornene)s, and therefore a discrepancy in the observed molecular weights can be expected as Grubbs' and coworkers have already reported.[19]

To demonstrate similar kinetic controlled mechanism works for **M2**, **G3** (1 equiv.), **CTA3** (50 equiv.) **M2** (1000 equiv.) and 3-bromopyridine (60 equiv.) were mixed in $CDCl_3$ in an NMR tube. The consumption of **M2** and **CTA3** were followed over time. Since **M2** has a higher propagation rate than **M1**, full consumption of **M2** was observed within 70 min and the conversion of **CTA3** was almost at 90% (Fig. 3D, Fig. S7‡). This, again, implied a kinetically controlled chain transfer mechanism even for **M2**.

To obtain insight into the structure–property relationships of monosubstituted 1,3 diene derivatives for catalytic ROMP, Hammett studies were performed using **CTA2**, **CTA3** and **CTA8** (Fig. S275‡). A negative reaction parameter (ρ = −0.88) indicated electron rich CTAs have higher reactivity and thus should be the choice of CTA for catalytic ROMP.

Branched ROMP polymers

Bifunctional CTAs. Many attempts to synthesize a bifunctional ruthenium complex have been reported in the literature that often required rigorous synthetic procedures, multi-step reaction conditions, complex purification, and low yield of the final ruthenium complex.[33] Above all, the polymerizations carried out using those complexes are non-catalytic and very often dependent on the use of particular monomers.[34] The Boydston group recently demonstrated bidirectional polymer growth in organocatalyzed ROMP from difunctional vinyl ether initiators using norbornene as the only monomer.[35]

Encouraged by the unusual reactivity of our regioselective CTAs, we synthesized **CTA11** carrying a long spacer between the two reacting sites. Then, a ^{1}H NMR experiment was performed to prove the pre-functionalization of **CTA11** on both sides (Fig. S8‡). Bifunctional **CTA12** was employed for the catalytic polymerization of both, **M1** and **M2** to obtain **P20** (**G3 : CTA12** = 1 : 50, $M_{n,\ SEC\ (CHCl3)}$ = 6.8 kDa) and **P24** (**G3 : CTA12** = 1 : 100, $M_{n,\ SEC\ (CHCl3)}$ = 7.7 kDa) with a good control over the molecular weights (Table S2‡). Since we could not rely on MALDI-ToF MS analyses to confirm the bidirectional growth of the polymers, additional support for the expected polymeric species was given by ^{1}H NMR spectroscopic data. There, we observed that upon polymerization, the conjugated double bonds of the initiator (CTA) shifted completely into the expected signals for the chain ends of the polymer (see ESI‡).

Star polymers. Having successfully carried out a catalytic bifunctional initiation of **M1** and **M2**, we hypothesized that higher functionality initiators should also be possible, leading to the formation of multi-arm star polymers (Fig. 4). Star polymers are a particular case of branched macromolecular architectures which contain at least three arms connected to one point, typically referred to as the "core".[36,37] Most synthetic methods for star polymers include living anionic polymerization, controlled/living radical polymerization[38] and ring-opening polymerization. ROMP can provide a wide variety of functional groups and benign experimental conditions, but still, there is no practical way to synthesize star-shaped ROMP polymers. Many attempts were made to synthesize star-shaped ROMP polymers that include using norbornene cross-linker,[39] dendritic multiarm ruthenium catalysts,[40] and in the recent past by synthesizing trifunctionalized Hoveyda-Grubbs' catalyst or Blechert's type catalyst.[41,42] However, all these examples require the synthesis of multi-functional initiators in stoichiometric amounts.

We first synthesized trifunctional **CTA13**. Then, a 100 times catalytic polymerization using **M1** (**M1 : CTA13** = 1 : 100) produced tri-arm star polymer, **P21**, with the molecular weight (4.6 kDa) controlled by the monomer (**M1**) to **CTA13** ratio. We then expanded our investigation further into catalytically synthesizing four-arm star polymers. **CTA14** was synthesized in three straightforward steps. A ^{1}H NMR tube polymerization employing **CTA14** and **M1** was performed to show full consumption of both **CTA14** and **M1**, suggesting a tetra functional growth (Fig. S10‡). In addition, SEC analysis of the resulting polymer **P22** provided a monomodal distribution with controlled $M_{n,\ SEC\ (CHCl3)}$ = 4.5 kDa ($M_{n,\ M1/CTA14}$ = 3.4 kDa). To further demonstrate the applicability of this method, a higher molecular weight tetra-arm star polymer **P23** ($M_{n,\ SEC\ (CHCl_3)}$ = 70 kDa) was also synthesized. Finally, **M3** was employed to obtain a four-arm functional star polymer (**P25**, **G3 : CTA14** = 1 : 64, $M_{n,\ SEC\ (CHCl_3)}$ = 6.5 kDa). A combination of SEC and ^{1}H NMR spectroscopy confirmed the expected star-shaped structure of the polymer. This straightforward route to making homo-arm star polymers is unique and highly efficient. To the best of our knowledge, this is the first report of synthesizing such complex polymeric architectures using a catalytic amount of ruthenium complex in metathesis chemistry.

A major drawback of our catalytic method is that molecular weight distribution or dispersity is relatively broad (1.45–2.10) due to a mechanistic necessity of a kinetically controlled catalytic polymerization. Nevertheless, the end-group fidelity of

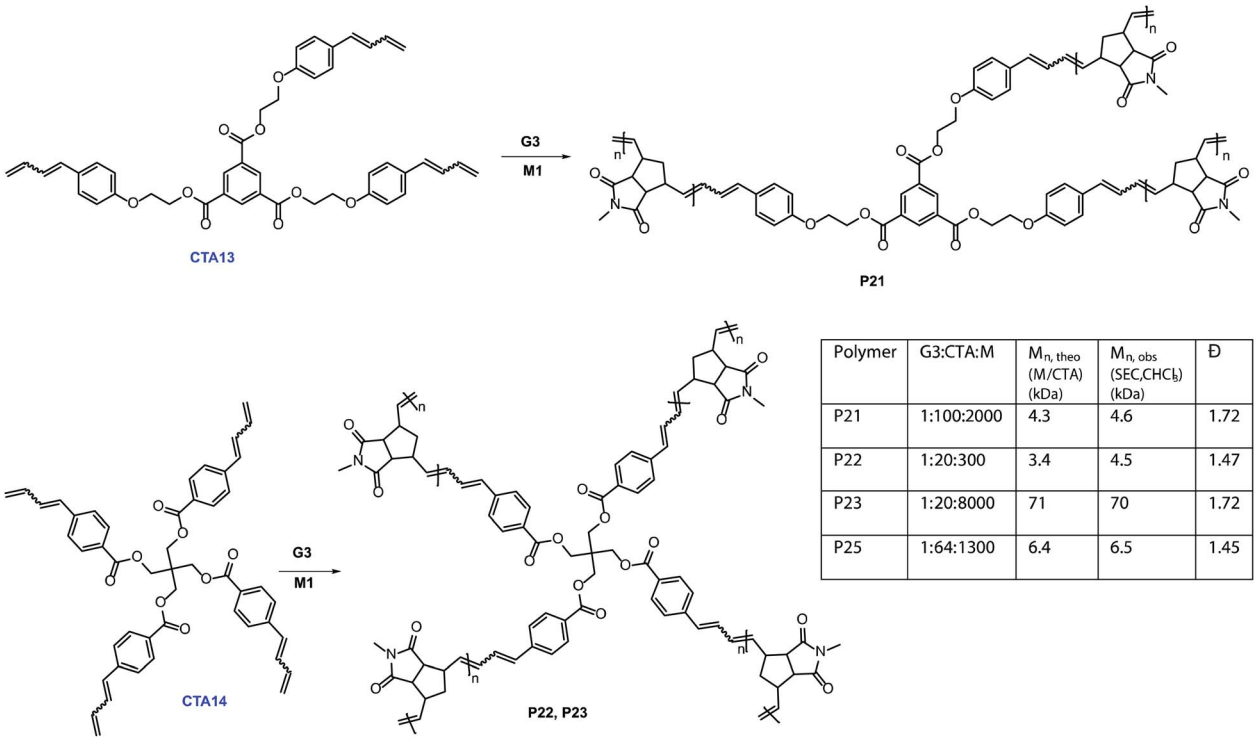

Polymer	G3:CTA:M	$M_{n,\ theo}$ (M/CTA) (kDa)	$M_{n,\ obs}$ (SEC,$CHCl_3$) (kDa)	Đ
P21	1:100:2000	4.3	4.6	1.72
P22	1:20:300	3.4	4.5	1.47
P23	1:20:8000	71	70	1.72
P25	1:64:1300	6.4	6.5	1.45

Fig. 4 Catalytic synthesis of three-arm and four-arm star polymers. Right inset: polymerization results for the synthesis of star-shaped polymers. M = Monomer, $Đ$ = dispersity.

polymer chain ends is always very high. Besides, recently it has been documented that both high and low dispersity polymers exhibit distinctive properties. In many cases, high dispersity polymeric materials are shown to be beneficial in different applications, including polymeric self-assembly, polymer blends' processability, and in different rheological properties.[43,44]

Disubstituted CTAs. In continuing our study of conjugated carbon–carbon double bonds in ruthenium-catalyzed metathesis, we were further interested in understanding how steric effects around the double bonds affect the reactivity and the regioselectivity. To gain additional insight, we studied disubstituted 1,3 dienes (**CTA15–26**) as CTAs. Due to an increase in steric congestion around the double bond, the reaction of these CTAs with **G3** was very sluggish. Moreover, the regioselective chain transfer was highly influenced by choice of the substituents (Fig. S13–33‡). Nevertheless, **CTA15** and **CTA17–19** were successfully used as a single functionalization agent to produce heterotelechelic metathesis polymers (Table S3‡) non-catalytically following the same mechanism described recently by our group.[45]

Interestingly, two sets of doublets were observed when (1*E*,3*E*,5*E*)-1,6-diphenylhexa-1,3,5-triene (**CTA26**) (see Fig. S37‡) was introduced to check the regioselectivity towards **G3**. Moreover, the end-capping experiment proved that non-regioselective chain transfer was involved in the case of sterically accessible triene derivatives (see Fig. S38 and S39‡).

Block copolymers. Catalytically synthesized end functional telechelic ROMP polymers could be advantageous for synthesizing block copolymers in combination with ATRP.[46–48] While a diblock copolymer was prepared straightforwardly, methods that included synthesizing the ROMP part of the block were always non-catalytic. This requires a very high loading of costly ruthenium complexes, making the overall block copolymer synthesis procedure unattractive.

ROMP-ATRP block copolymer. A chain transfer agent carrying an ATRP initiator group could allow for the synthesis of ROMP-ATRP block copolymers on a gram scale. α-Bromoester (ATRP initiator) functionalized **CTA9** produced a monotelechelic polymer **P13** catalytically. **P13** was then used as a macroinitiator to grow a poly(styrene) block using the CuBr/PMDETA catalyst system in bulk at 95 °C. Fig. 5A shows the SEC traces of homopolymer **P13** (blue line, $M_{n,\ SEC\ (CHCl3)} = 8.0$ kDa, $Đ = 1.77$) and block copolymer **P13-b-PS** (red line, $M_{n,\ SEC\ (CHCl3)} = 19.4$ kDa, $Đ = 1.29$). A monomodal peak of the final block copolymer was observed, which suggested complete initiation of the α-bromoester moiety. DOSY NMR spectroscopy further supported the successful synthesis of block copolymer (Fig. S167‡). Our catalytic ROMP method in conjugation with ATRP could be further used to synthesize multiblock copolymers in a greener and more cost-effective way.

Block copolymer by NCL. Native chemical ligation (NCL) is a widely accepted method for synthesizing peptides and proteins.[49] This ligation technique is highly efficient, often high yielding, and can be performed under mild conditions. Despite all this, there are limited literature reports regarding ligation between two synthetic polymers.[50] Inspired by the efficiency and speed of NCL to produce block copolymers,[51] here, we report an

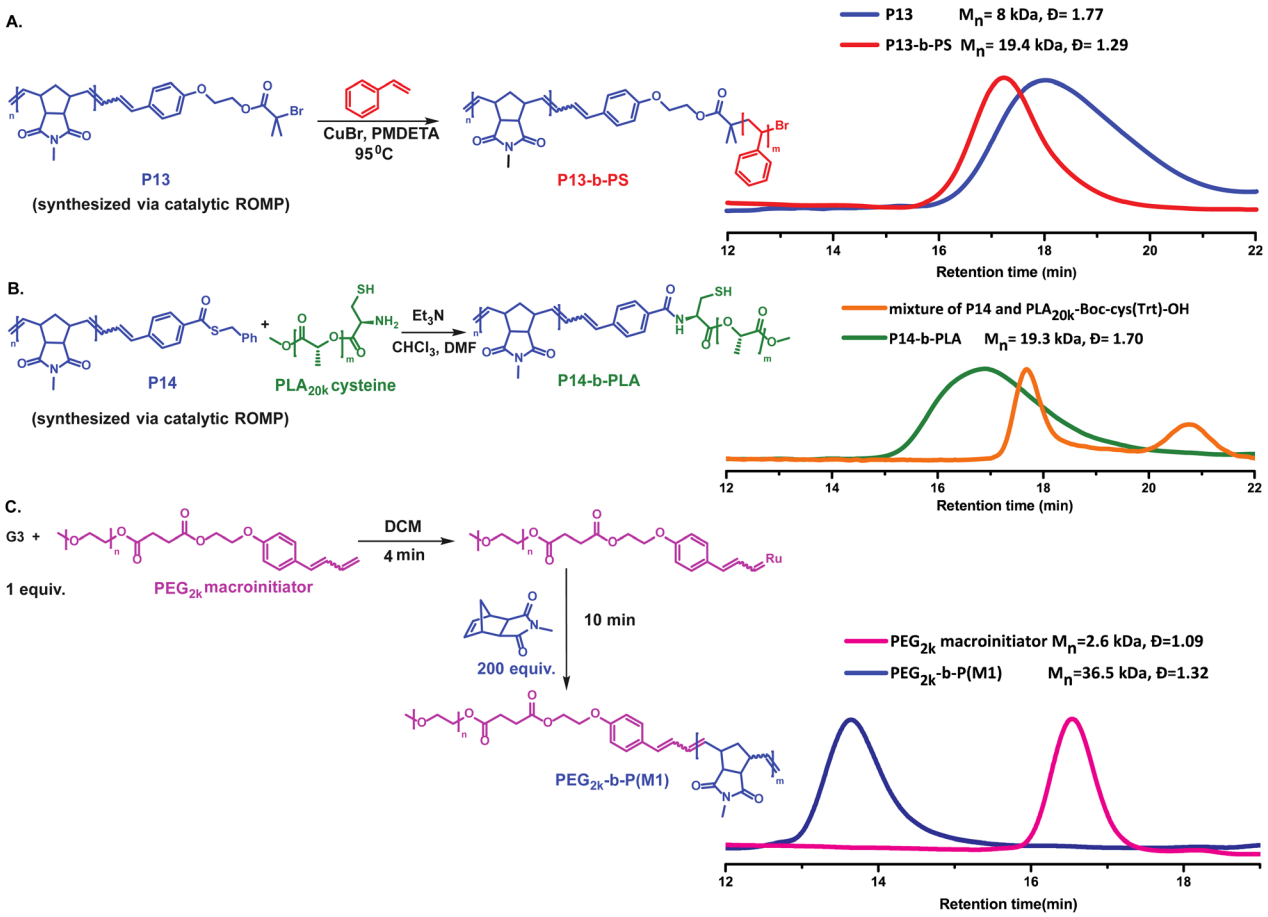

Fig. 5 Synthesis of block copolymers. (A) Synthesis of **P13-b-PS** diblock copolymer *via* catalytic ROMP followed by ATRP and SEC ($CHCl_3$) characterization. (B) NCL synthesis of the diblock copolymer **P14-b-PLA** and SEC ($CHCl_3$) characterization. (C) Synthesis of diblock copolymer **PEG_{2k}-b-P(M1)** *via* macroinitiation from a poly(ethylene glycol) macroinitiator (PEG_{2k} macroinitiator) and SEC (DMF) characterization.

economical, atom-efficient way to make such polymers under very mild reaction conditions. Commercially available poly(L-lactide) (PLA, M_n = 20 kDa, $Đ$ = 1.08) was end-functionalized with cysteine using a protection and deprotection strategy (see ESI‡). We synthesized thioester end functional ROMP polymer **P14** (see above) catalytically. Then, both polymers were mixed in a chloroform and dimethylformamide solvent mixture, followed by adding a few drops of triethylamine to give PLA-ROMP diblock copolymer, **P14-b-PLA** ($M_{n,\ SEC\ (CHCl3)}$ = 19.3 kDa, $Đ$ = 1.70). To confirm the formation of the block copolymer, SEC was measured of both polymers before and after coupling (Fig. 5B). A bimodal distribution was observed before coupling, which transformed into a monomodal distribution after NCL. Besides, the DOSY spectrum of the diblock copolymer showed a single diffusing species after the coupling reaction compared to two distinctive signals observed when both polymers were mixed before coupling (Fig. S172 and S173‡). Both SEC and DOSY NMR spectroscopy strongly indicated the formation of the diblock copolymer.

Macroinitiation *via* ROMP. So far, there have been very few reports to grow ROMP polymers from a macromolecule using olefin metathesis catalysts.[52–54] Functionalizing any metathesis catalyst using only one equivalent pre-functionalization agent attached to a polymer is exceedingly challenging. Given the speed and high regioselectivity of our CTAs, we anticipated that a monosubstituted 1,3 diene derivative attached to the chain end of a polymer could serve as a macroinitiator to initiate ROMP. Poly(ethylene glycol) (PEG) based macroinitiator, PEG_{2k} macroinitiator ($M_{n,\ SEC\ (DMF)}$ = 2.6 kDa, $Đ$ = 1.09) bearing a conjugated double bond was synthesized in a few steps and analyzed fully with SEC, ^{1}H NMR spectroscopy, and MALDI-ToF mass spectrometry (see ESI‡). A stock solution of both PEG_{2k} macroinitiator and **G3** was prepared and mixed equimolarly (see ESI‡). After five minutes, a solution of **M1** in degassed dichloromethane was quickly added to the previous mixture. Within ten minutes, all the monomer was consumed (confirmed *via* ^{1}H NMR spectroscopy), and the polymerization was terminated by adding a few drops of ethyl vinyl ether. SEC elugram of both PEG_{2k} macroinitiator (first block, $M_{n,\ SEC\ (DMF)}$ = 2.6 kDa, $Đ$ = 1.09) and block copolymer, **PEG_{2k}-b-P (M1)** (diblock, $M_{n,\ SEC\ (DMF)}$ = 36.5 kDa, $Đ$ = 1.32) are shown in Fig. 5C. The complete disappearance of the PEG_{2k} macroinitiator (first block) signal was observed in the SEC chromatogram along with a significant increase in the molecular weight of the final diblock copolymer suggesting a highly efficient macroinitiation. This method highlights a very rapid and

straightforward technique to prepare ROMP-based diblock copolymers *via* the macroinitiation approach. We believe that using this approach, many other types of diblock copolymers such as poly(lactide)-ROMP, poly(dimethyl siloxane)-ROMP, and so on could be synthesized with ease.

Conclusions

In conclusion, we have successfully designed a simple yet efficient synthetic method to prepare ROMP polymers catalytically in a one-pot approach using a new type of chain transfer agents. The total polymerization time is typically less than fifteen minutes which emphasizes the ultrafast kinetics of the reported CTAs. Various substituents are introduced selectively at one terminus of the polymer chain producing monotelechelic polymers in a catalytic fashion. The catalyst to CTA ratio studied in this report was as low as 1 to 300, meaning a 300-fold saving of costly and toxic ruthenium carbene complex. Complex polymeric architectures such as homo-arm star polymers have been synthesized catalytically using a core-first approach for the first time in metathesis-based polymerization. Telechelic polymers obtained *via* our method were further employed to produce block copolymers using orthogonal chemistry like ATRP and NCL. Moreover, a macroinitiation approach was introduced to prepare ROMP block polymers.

The development of catalytic ring opening metathesis polymerization methods is an ongoing effort. It reduces the cost of expensive metathesis-based catalysts and offers considerable potential for synthesizing functional ROMP polymers for biomedical or materials uses where lower contaminations of toxic ruthenium metal are critical. The current environmentally friendly approach can be used to synthesize end functional homopolymers, block copolymers, and other complex architectures that could lead to new applications in industrial and materials chemistry.

Data availability

We have included all data in the ESI section.‡

Author contributions

I. M and A. F. M. K designed the experiments. A. M synthesized PLA_{20k}-cysteine and **P31-b-PLA**. M. A. R performed a few MALDI-ToF MS analyses. I. M carried out the rest of the syntheses, analyses, and kinetic studies. I. M and A. F.M. K. wrote the manuscript. All authors reviewed the manuscript.

Conflicts of interest

There are no conflicts to declare.

Acknowledgements

A. F. M. K, I. M, A. M, M. A. R thanks Swiss National Science Foundation, National Center of Competence in Research (NCCR Bio-inspired Materials) and the Fribourg Center for Nanomaterials (FriMat) for support. We also acknowledge Dr Krzysztof Piech, Rahul Giri and Subrata Patra for their kind help during GC-MS measurements and analyses.

Notes and references

1 S. Sutthasupa, M. Shiotsuki and F. Sanda, *Polym. J.*, 2010, **42**, 905–915.
2 Y. Chen, M. M. Abdellatif and K. Nomura, *Tetrahedron*, 2018, **74**, 619–643.
3 M. R. Buchmeiser, *Chem. - Eur. J.*, 2018, **24**, 14295–14301.
4 O. M. Ogba, N. C. Warner, D. J. O'Leary and R. H. Grubbs, *Chem. Soc. Rev.*, 2018, **47**, 4510–4544.
5 M. S. Sandford, J. A. Love and R. H. Grubbs, *J. Am. Chem. Soc.*, 2001, **123**, 6543–6554.
6 T. M. Trnka and R. H. Grubbs, *Acc. Chem. Res.*, 2001, **34**, 18–29.
7 T. L. Choi and R. H. Grubbs, *Angew. Chem., Int. Ed.*, 2003, **42**, 1743–1746.
8 C. W. Bielawski and R. H. Grubbs, *Prog. Polym. Sci.*, 2007, **32**, 1–29.
9 J. B. Matson and R. H. Grubbs, *Macromolecules*, 2010, **43**, 213–221.
10 S. Hilf and A. F. M. Kilbinger, *Nat. Chem.*, 2009, **1**, 537–546.
11 A. F. M. Kilbinger, *Synlett*, 2019, **30**, 2051–2057.
12 S. Pal, F. Lucarini, A. Ruggi and A. F. M. Kilbinger, *J. Am. Chem. Soc.*, 2018, **140**, 3181–3185.
13 B. R. Elling and Y. Xia, *ACS Macro Lett.*, 2018, **7**, 656–661.
14 L. Fu, T. Zhang, G. Fu and W. R. Gutekunst, *J. Am. Chem. Soc.*, 2018, **140**, 12181–12188.
15 P. Liu, M. Yasir, A. Ruggi and A. F. M. Kilbinger, *Angew. Chem.*, 2018, **130**, 926–929.
16 M. A. Hillmyer and R. H. Grubbs, *Macromolecules*, 1993, **26**, 872–874.
17 M. A. Hillmyer and R. H. Grubbs, *Macromolecules*, 1995, **28**, 8662–8667.
18 M. A. Hillmyer, S. T. Nguyen and R. H. Grubbs, *Macromolecules*, 1997, **30**, 718–721.
19 C. W. Bielawski, D. Benitez, T. Morita and R. H. Grubbs, *Macromolecules*, 2001, **34**, 8610–8618.
20 M. Yasir, P. Liu, I. K. Tennie and A. F. M. Kilbinger, *Nat. Chem.*, 2019, **11**, 488–494.
21 P. Liu, M. Yasir and A. F. M. Kilbinger, *Angew. Chem., Int. Ed.*, 2019, **58**, 15278–15282.
22 V. C. Gibson and T. Okada, *Macromolecules*, 2000, **33**, 655–656.
23 J. B. Matson, S. C. Virgil and R. H. Grubbs, *J. Am. Chem. Soc.*, 2009, **131**, 3355–3362.
24 T. Zhang and W. R. Gutekunst, *Polym. Chem.*, 2020, **11**, 259–264.
25 A. Mandal, I. Mandal and A. F. M. Kilbinger, *ACS Macro Lett.*, 2022, 491–497.
26 H. Katayama, H. Urushima and F. Ozawa, *Chem. Lett.*, 1999, **28**, 369–370.
27 H. Katayama, F. Yonezawa, M. Nagao and F. Ozawa, *Macromolecules*, 2002, **35**, 1133–1136.

28 H. Katayama, Y. Fukuse, Y. Nobuto, K. Akamatsu and F. Ozawa, *Macromolecules*, 2003, **36**, 7020–7026.
29 J. Louie and R. H. Grubbs, *Organometallics*, 2002, **21**, 2153–2164.
30 P. Schwab, R. H. Grubbs and J. W. Ziller, *J. Am. Chem. Soc.*, 1996, **118**, 100–108.
31 E. K. Riga, D. Boschert, M. Vöhringer, V. T. Widyaya, M. Kurowska, W. Hartleb and K. Lienkamp, *Macromol. Chem. Phys.*, 2017, **218**, 1700273.
32 A. E. Madkour, A. H. R. Koch, K. Lienkamp and G. N. Tew, *Macromolecules*, 2010, **43**, 4557–4561.
33 K. Grudzień, M. Malinska and M. Barbasiewicz, *Organometallics*, 2012, **31**, 3636–3646.
34 V. Komanduri, D. R. Kumar, D. J. Tate, R. Marcial-Hernandez, B. J. Lidster and M. L. Turner, *Polym. Chem.*, 2019, **10**, 3497–3502.
35 P. Lu, N. M. Alrashdi and A. J. Boydston, *J. Polym. Sci., Part A: Polym. Chem.*, 2017, **55**, 2977–2982.
36 J. M. Ren, T. G. McKenzie, Q. Fu, E. H. H. Wong, J. Xu, Z. An, S. Shanmugam, T. P. Davis, C. Boyer and G. G. Qiao, *Chem. Rev.*, 2016, **116**, 6743–6836.
37 K. Khanna, S. Varshney and A. Kakkar, *Polym. Chem.*, 2010, **1**, 1171.
38 K. Matyjaszewski and J. Xia, *Chem. Rev.*, 2001, **101**, 2921–2990.
39 R. S. Saunders, R. E. Cohen, S. J. Wong and R. R. Schrock, *Macromolecules*, 1992, **25**, 2055–2057.
40 S. Gatard, S. Nlate, E. Cloutet, G. Bravic, J.-C. Blais and D. Astruc, *Angew. Chem., Int. Ed.*, 2003, **42**, 452–456.
41 C. Zhou, C. Hou and J. Cheng, *Polym. Chem.*, 2020, **11**, 1735–1741.
42 K. O. Kim, S. Shin, J. Kim and T.-L. Choi, *Macromolecules*, 2014, **47**, 1351–1359.
43 R. Whitfield, K. Parkatzidis, N. P. Truong, T. Junkers and A. Anastasaki, *Chem*, 2020, **6**, 1340–1352.
44 N. A. Lynd, A. J. Meuler and M. A. Hillmyer, *Prog. Polym. Sci.*, 2008, **33**, 875–893.
45 A. Mandal, I. Mandal and A. F. M. Kilbinger, *ACS Macro Lett.*, 2021, **10**, 1487–1492.
46 C. Cheng, E. Khoshdel and K. L. Wooley, *Nano Lett.*, 2006, **6**, 1741–1746.
47 J. B. Matson and R. H. Grubbs, *Macromolecules*, 2008, **41**, 5626–5631.
48 C. W. Bielawski, T. Morita and R. H. Grubbs, *Macromolecules*, 2000, **33**, 678–680.
49 V. Agouridas, O. El Mahdi, V. Diemer, M. Cargoët, J.-C. M. Monbaliu and O. Melnyk, *Chem. Rev.*, 2019, **119**, 7328–7443.
50 A. Rajakanthan, P. A. J. M. de Jongh, J. S. Town, P. Wilson and K. Kempe, *Polym. Chem.*, 2019, **10**, 5242–5250.
51 S. Pal, A. Mandal, L. Hong, R. D. Ortuso, A. Petri-Fink, S. Salentinig and A. F. M. Kilbinger, *Macromolecules*, 2022, **55**, 2854–2860.
52 T. C. Castle, L. R. Hutchings and E. Khosravi, *Macromolecules*, 2004, **37**, 2035–2040.
53 S. Pal, I. Mandal and A. F. M. Kilbinger, *ACS Macro Lett.*, 2022, 847–853.
54 A. Mandal, I. Mandal and A. F. M. Kilbinger, *Macromolecules*, 2022, **55**, 7827–7833.